Geometric Wave Engineering.
Theory of Higher-Order Pseudoparaboloids.
Volume 1.
Constructive Geometry:
Recursive Constructions and Computational Apparatus

Vladimir Igorevich Khaustov
Independent Researcher
ORCID: 0009-0007-3657-2309
DOI: 10.5281/zenodo.20022183
Research project: https://vihrihaosa.ru/

04.05.2026

Abstract

This work introduces and formalizes a family of axially symmetric domains — higher-order pseudoparaboloids Ω_n and their row stackings Ω_{n,m} — generated by a recursive interval construction over vertical and horizontal parabolic generatrices with focal parameter f and limiting radius R. The construction is realized as iterations of the operator C_R acting on the space $\mathcal{I}([0,\infty))$ of nonempty finite unions of closed intervals, followed by the canonical Merge operation that guarantees correctness of the area and volume functionals of the cross-sections. We establish the basic geometric properties: nonnegativity and the explicit upper bound $M_n \le M_0 + \Sigma_{k=1}^{n-2} R_k$, where M_0=max d and in the standard vertical base case M_0=R; closedness and compactness of Ω_n and Ω_{n,m} for any finite order n and finite row number m; piecewise smoothness of the generatrix with a finite number of break points and finite cross-sectional area near the axial vertex; and a connectedness criterion expressed through the intersection graph of the generated intervals. Closed-form expressions for the focal points of the generated parabolic arcs of arbitrary finite order are derived and verified numerically on the reference example (f = 2, R = 8, R_1 = 7, R_2 = 14, n = 4). The computational implementation is treated as a reproducible Python reference for the geometry. Physical hypotheses (modal confinement, spectral signatures, quality factor) are explicitly deferred to the subsequent wave-verification programme and are not claimed in the present volume.

Keywords: *geometric wave engineering; constructive geometry; pseudoparaboloid;interval recursion; Merge operation; axially symmetric row stacking; Gaussian and mean curvature; compactness; reproducible implementation.*

DOI: 10.5281/zenodo.20022183 Zenodo Publication

ORCID: 0009-0007-3657-2309 Date: 04.05.2026

Contents

DOI: 10.5281/zenodo.20022183 Zenodo Publication

ORCID: 0009-0007-3657-2309 Date: 04.05.2026

Chapter 1. Subject, object, and scientific status of the theory

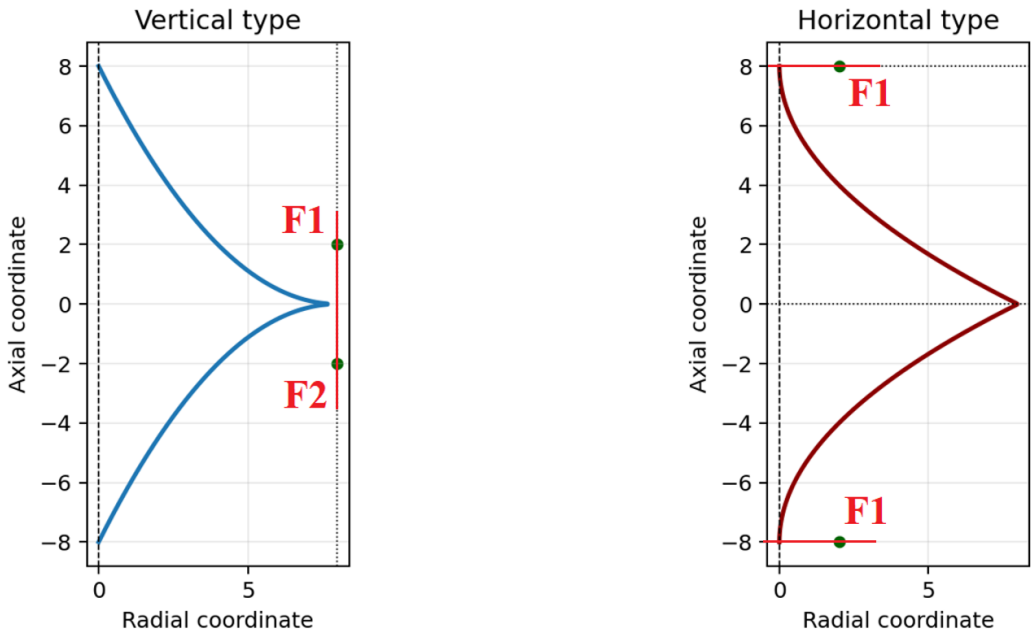

Fig. 1. Base parabolic generatrices of the vertical and horizontal types.

1.1. Main object

This volume introduces the constructive geometry of higher-order pseudoparaboloids as an independent mathematical and computational apparatus of Geometric Wave Engineering. The main object of the theory is not an individual line, not an illustration, and not a set of surfaces, but the unified internal volume Ω_{n,m} generated by a parabolic generatrix, interval recursion, the Merge operation, and row-wise axial assembly.

The theory in this volume prepares the geometry for further physical validation. It does not declare localization, confinement, directed output, or universal wave control to be proven in advance. These effects are treated as testable hypotheses to be verified by ray dynamics, the Helmholtz equation, acoustics, electromagnetic FEM/FDTD models, and later by experiment.

Unlike a purely visual description, the volume formally defines the state space of interval geometry, the recursion operator, Merge, boundedness, compactness, connectedness, curvature, singularities, and analytic foci of generating parabolic arcs. Figures are used only as control visualizations of formulas.

Definition 1.1. Pseudoparaboloid of finite order.

A pseudoparaboloid of order n with parameters (f, R, R_1, …, R_{n−2}) is an axially symmetric domain $\Omega_n \subset \mathbb{R}^3$ obtained by rotation about the axis e_ξ of the planar set {(ξ,ρ): ρ ∈ I_n(ξ)}, where I_2(ξ)=[0,d(ξ)] and I_n is defined by the recursive interval construction and subsequent Merge operation. The term “pseudo-” indicates that Ω_n is not the standard paraboloid of revolution but a recursively generated axisymmetric domain whose boundary is assembled from parabolic arcs, reflected or shifted parabolic copies, and Merge-selected visible components.

DOI: 10.5281/zenodo.20022183 Zenodo Publication

ORCID: 0009-0007-3657-2309 Date: 04.05.2026

1.2. From generatrix to volume

The base parabolic generatrix defines the distance d(ξ) from the axis of rotation to the second-order boundary. At the second order the internal radial interval is I_2(ξ)={[0,d(ξ)]}. At subsequent levels each interval is transformed by the operator C_R, and intersecting or touching intervals are then united by the Merge operator. Rotation around the axis gives the spatial domain Ω_n; row assembly gives Ω_{n,m}.

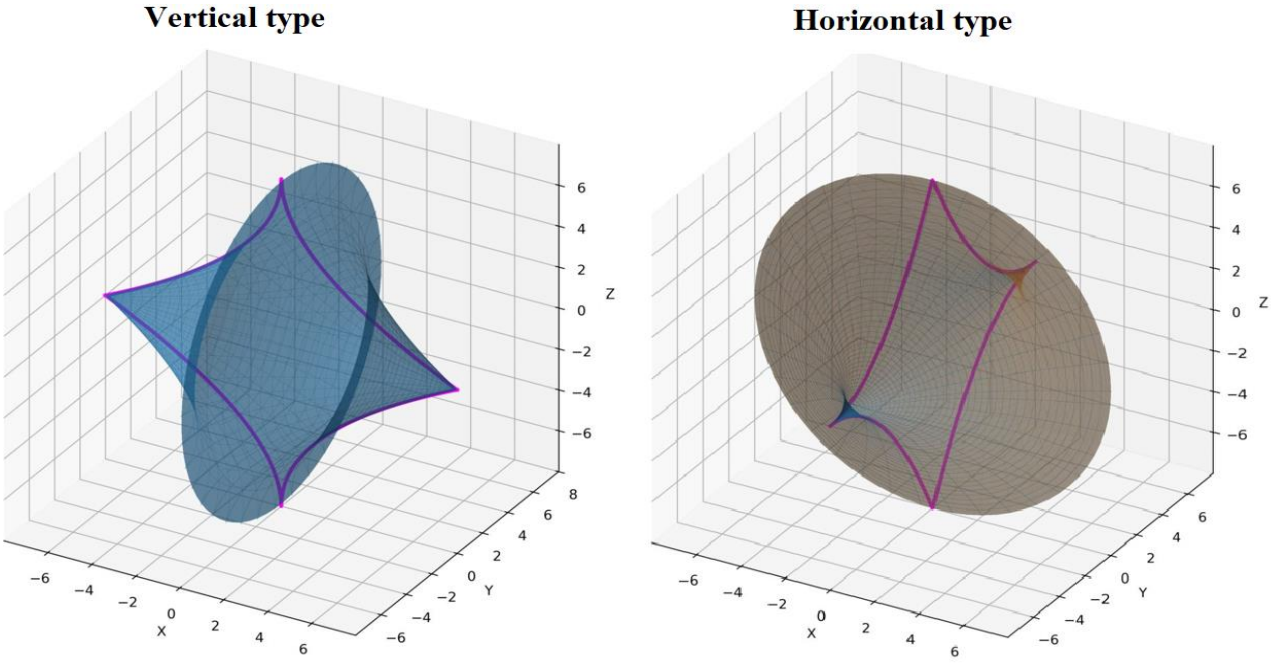

Fig. 2. Construction of 3D second-order surfaces.

1.3. Methodological separation between theory and visualization

A geometric statement belongs to the theory only when it is expressed by a formula, lemma, theorem, definition, or computable functional. Visualization does not replace proof: it only shows a form already defined analytically or algorithmically.

Therefore parameter and regime tables are introduced once and then used without repetition. Figures do not duplicate one another: each figure answers a distinct theoretical question - base generatrix, recursion, order, 3D boundary, curvature, singularity, row assembly, or numerical example.

$$\Omega_{n,m}=\bigcup_{j=0}^{m-1}(\Omega_n+\Delta_j e_\xi)$$

Table 1. Main levels of description

Level	Object	Purpose
Generatrix	d_v, d_h	defines the second order
Intervals	I_n(ξ)	define radial zones
Volume	Ω_n, Ω_{n,m}	computational domain
Script	Python	reproduces constructions

DOI: 10.5281/zenodo.20022183 Zenodo Publication

ORCID: 0009-0007-3657-2309 Date: 04.05.2026

Chapter 2. Base parabolic geometry

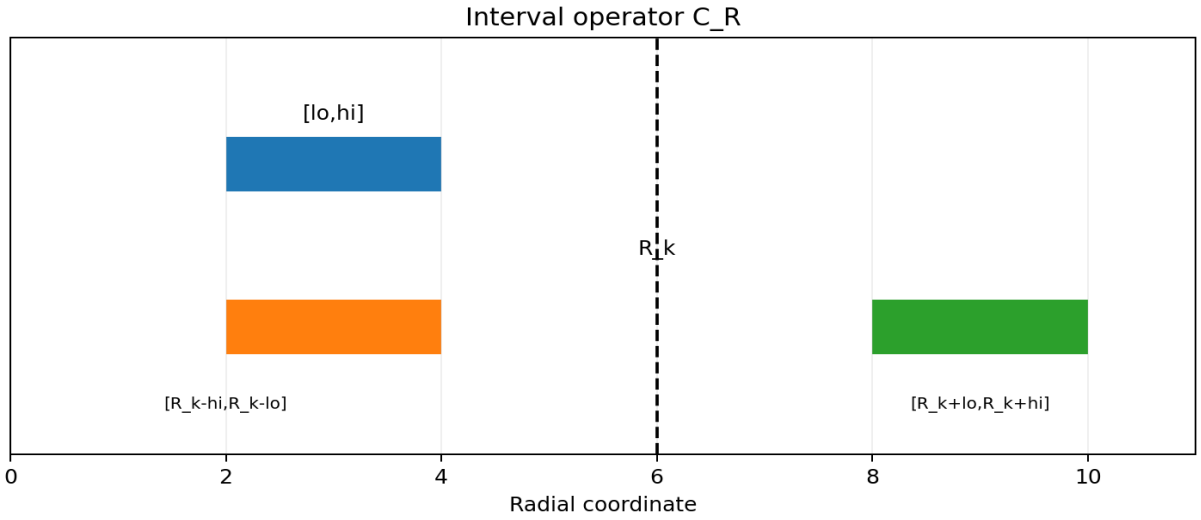

Fig. 3. Action of the interval operator C_R.

2.1. Vertical and horizontal types

The vertical type is built from two mirrored parabolic branches joined at a common vertex on the focal line. For a focal parameter $f>0$ and distance $R>0$ to the axis of rotation, the base half-length is $a=R^2/(4f)$. The radial distance to the generatrix is $d_v(s)=R-2\sqrt{(f|s|)}$, $0\le|s|\le a$.

The horizontal type is a rotated realization of the same parabolic principle and is defined by $d_h(u)=(R-|u|)^2/(4f)$, $|u|\le R$. Formally the recursive apparatus is identical for both types; the base function, axis of rotation, focus positions, and singularities differ.

2.2. Second order as an internal volume

The second order is not only a surface of revolution. At each admissible axial coordinate there exists the full radial interval $0\le\rho\le d(\xi)$. This interval, not only the boundary curve, is passed into recursion. If one considers only the boundary curve $\rho=d(\xi)$, the computational domain required for later wave problems is lost.

$$a=R^2/(4f)$$

$$d_v(s)=R-2\sqrt{(f|s|)},\ \ 0\le|s|\le a$$

$$d_h(u)=(R-|u|)^2/(4f),\ \ |u|\le R$$

$$I_2(\xi)=\{[0,d(\xi)]\}$$

2.3. Relation to classical parabolic objects

The present construction is related to the standard paraboloid of revolution but is not identical to it. At $n=2$, before any recursive offsets are applied, the boundary is generated directly from the chosen parabolic generatrix and the internal volume is represented by the interval $I_2(\xi)=[0,d(\xi)]$. Thus the second order is the classical parabolic base domain in the sense of the selected vertical or horizontal generatrix.

DOI: 10.5281/zenodo.20022183 Zenodo Publication

ORCID: 0009-0007-3657-2309 Date: 04.05.2026

For n≥3 the family {Ω_n} generalizes the parabolic base by introducing recursive radial offsets R_k, clipping to admissible radii, and Merge. In the degenerate case R_1=0 the first recursive step does not create a genuinely new radial offset; in the non-degenerate case R_1>0 the third and higher orders form shifted or reflected parabolic boundary copies. Therefore the construction should be read as a recursive extension of parabolic domains, not as a redefinition of the classical paraboloid itself.

Table 2. Parameters of the base geometry

Symbol	**Meaning**
f	focal distance of a parabolic branch
R	distance from the rotation axis to the focal line / scale
a	half-length of the vertical type and characteristic size
d(ξ)	radial distance to the generatrix

DOI: 10.5281/zenodo.20022183 Zenodo Publication

ORCID: 0009-0007-3657-2309 Date: 04.05.2026

Chapter 3. Interval algebra and the Merge operator

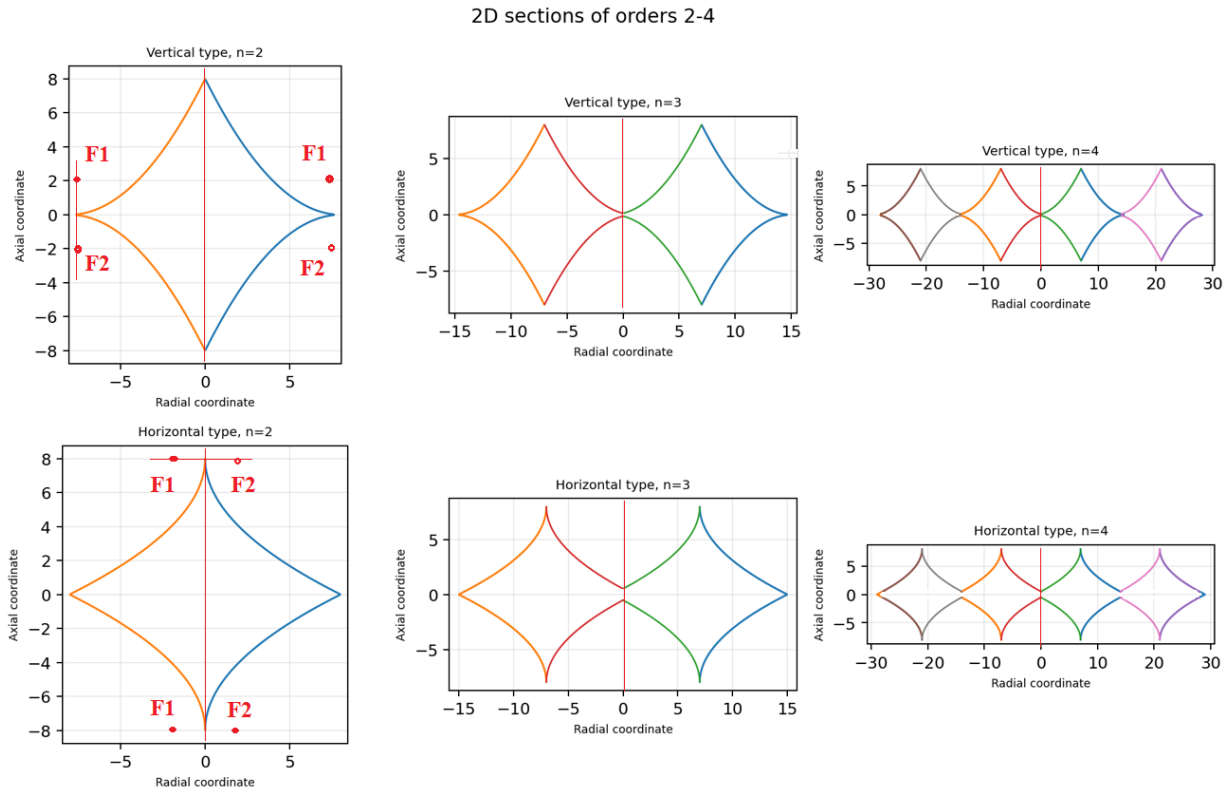

Fig. 4. 2D sections of orders 2, 3 and 4 after Merge.

3.1. State space

Let $\mathcal{I}([0,\infty))$ be the set of all finite unions of closed bounded intervals on the half-line $[0,\infty)$. An element of this space is written as a finite family of disjoint intervals $[\alpha_j,\beta_j]$ with $0\le\alpha_j\le\beta_j$. At each axial point ξ the pseudoparaboloid object is described by such an element of $\mathcal{I}$.

For one interval [lo,hi], the order operator with parameter R produces two intervals: a difference interval and a sum interval. Merge is then applied - transition to the canonical representation of the union without duplicated parts.

3.2. Lemma on correctness of Merge

Lemma 3.1. Let S be a finite family of closed bounded intervals on $[0,\infty)$. Then Merge(S), obtained by sorting the intervals and uniting intersecting or touching pairs, is a finite family of pairwise disjoint closed bounded intervals and represents the same point set as the original union.

Proof. A finite union of compact intervals is compact. Sorting by the left endpoint allows one to unite only those intervals whose left endpoints do not exceed the current right endpoint. After the algorithm terminates, a positive gap exists between neighboring intervals, so they are disjoint. No point is lost or added, because each operation replaces $A\cup B$ by the minimal interval equal to this union when A and B intersect or touch.

DOI: 10.5281/zenodo.20022183 Zenodo Publication

ORCID: 0009-0007-3657-2309 Date: 04.05.2026

3.3. Lemma on 1-Lipschitz mappings

Lemma 3.2. For any $R \geq 0$ the mappings $g_R(r)=\max(R-r,0)$ and $h_R(r)=R+r$ are 1-Lipschitz on $[0,\infty)$, with h_R being an isometric shift with the same constant. For g_R one has $|g_R(r_1)-g_R(r_2)| \leq |r_1-r_2|$.

Proof. The function $q(r)=R-r$ is an orientation-reversing isometry, and $p(x)=\max(x,0)$ is the metric projection onto $[0,\infty)$, hence does not increase distances. The composition $p \circ q$ therefore does not increase distances. For h_R, $|(R+r_1)-(R+r_2)|=|r_1-r_2|$ is immediate.

$$C_R([lo,hi])=[\max(R-hi,0), \max(R-lo,0)] \cup [R+lo, R+hi]$$

$$I_{k+1}(\xi)=\mathrm{Merge}(\bigcup_{[\alpha,\beta]\in I_k(\xi)} C_{R_k}([\alpha,\beta]))$$

Table 3. Status of interval operations

Operation	Mathematical status
C_R	mapping $\mathcal{I} \to \mathcal{I}$
Merge	canonicalization of a finite union
$\max(\cdot,0)$	projection to admissible radii

Additional remarks

Lemma 3.2 implies continuity of C_R in the Hausdorff metric on single intervals. For finite unions of intervals this continuity is preserved componentwise up to contact events and Merge re-indexing. This is why the numerical visualization may change the number of displayed components without changing the unified set itself.

Stabilization of the sequence I_k as $k \to \infty$ is not guaranteed for arbitrary positive offsets. A sufficient condition for a bounded limiting set is summability of offsets $\Sigma R_k < \infty$ together with closure in the Hausdorff metric after Merge. For constant R_k the radial radius generally grows linearly, so no compact limiting set arises without additional normalization. This statement concerns only the limiting process $k \to \infty$. For every finite order n, the constructed domain remains bounded and compact by Theorem 4.2.

DOI: 10.5281/zenodo.20022183 Zenodo Publication

ORCID: 0009-0007-3657-2309 Date: 04.05.2026

Chapter 4. Theorems on the properties of Ω_n and Ω_{n,m}

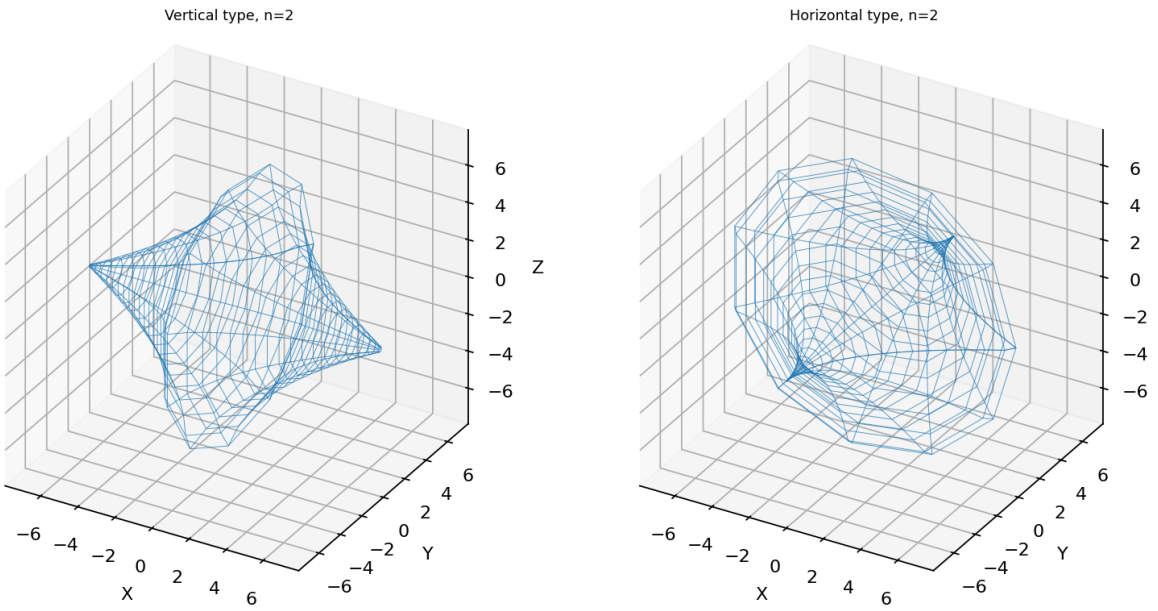

Fig. 5. 3D surfaces of the second order.

4.1. Non-negativity and boundedness

Theorem 4.1. For any f>0, R>0 and any non-negative recursive offsets R_k, all intervals appearing in the recursion have non-negative endpoints. Moreover, if M_0=max d, then the upper radius of any interval of order n does not exceed M_0+Σ_{k=1}^{n−2}R_k.

Proof. At the second order the intervals are [0,d], where d≥0. If [lo,hi]⊂[0,M], the clipped difference interval has non-negative endpoints, and the sum interval lies in [R_k,R_k+M]. Therefore the new maximum radius does not exceed R_k+M. Induction over k gives the stated bound.

4.2. Compactness

Theorem 4.2. For any finite n, finite m, and finite parameters f, R, R_k, h, the domain Ω_{n,m} is a bounded closed domain in $\mathbb{R}^3$, except that its boundary may be only piecewise smooth. This is a finite-order statement and does not assert compactness of an infinite-order limit without additional normalization.

Proof. The axial domain of each instance is bounded. Radii are bounded by Theorem 4.1. At a fixed axial coordinate, Merge gives a finite union of closed intervals. Rotation of a closed radial set around the axis preserves closedness, and a finite union of rows is also closed. Boundedness follows from finite axial shifts and the radial estimate.

4.3. Connectedness for one recursive step and sufficient conditions

Theorem 4.3. If, at a fixed ξ, the current section is a single interval [0,M(ξ)] and R_k≤M(ξ), then after applying C_{R_k} and Merge the new section is again a single interval [0,R_k+M(ξ)]. If

DOI: 10.5281/zenodo.20022183 Zenodo Publication
ORCID: 0009-0007-3657-2309
Date: 04.05.2026

R_k>M(ξ), the new section formally becomes [R_k−M(ξ),R_k]∪[R_k,R_k+M(ξ)], which touches at R_k and therefore Merge again gives a single interval [R_k−M(ξ),R_k+M(ξ)]. However, for an initial interval [α,β] with α>0, two separated rings occur precisely when the right endpoint of the clipped difference interval lies below the left endpoint of the sum interval, i.e. when R_k−β>α, equivalently R_k>α+β. If R_k−β≤α, the two generated intervals intersect or touch and Merge gives one interval.

Corollary. Global connectedness of Ω_n is not determined by the single inequality R_k≤M_{k−1}; it depends on the axial domain, on the presence of intervals with positive lower endpoints, and on Merge between neighboring components. Therefore, in the general case the correct result is not a simple equivalence but a local-sectional connectedness classification.

$$M_n \le M_0 + \Sigma R_k$$

$$A_n(\xi) = \pi \Sigma_j (\beta_j^2 - \alpha_j^2)$$

Table 4. Established properties of Ω

Property	Status
Non-negative radii	theorem
Boundedness	theorem
Closedness after Merge	theorem
Global connectedness	local classification, not a universal equivalence

Connectedness and component graph

For a full global classification of connectedness, one constructs a component graph: vertices correspond to Merge intervals on axial segments, and edges correspond to continuation of these components as ξ changes. This graph formulation naturally leads to C1–C8 classifications in subsequent work.

DOI: 10.5281/zenodo.20022183 Zenodo Publication

ORCID: 0009-0007-3657-2309 Date: 04.05.2026

Chapter 5. Branch core and IFS interpretation

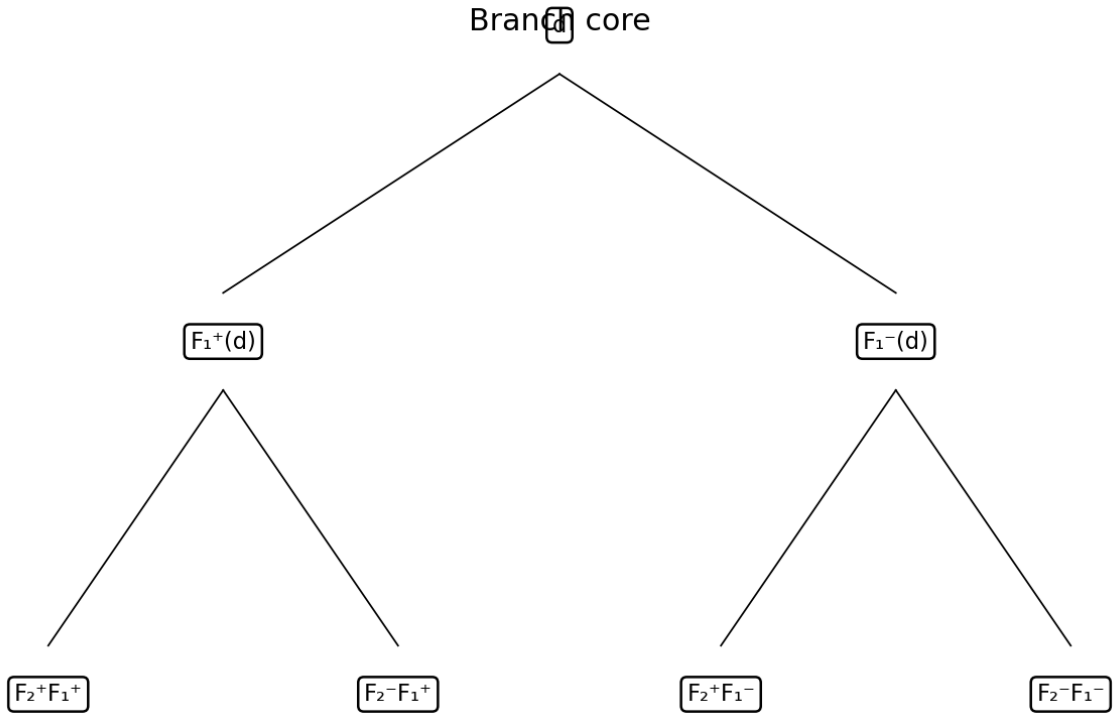

Fig. 6. Branch core as a finite orbit of affine mappings.

5.1. Formal branch tree

The branch core is generated by mappings F_k^+(r)=R_k+r and F_k^−(r)=R_k−r. The cardinality of the branch core B_n, before clipping and before Merge, equals 2^{n−2}. This number is not the number of physical components after Merge: intersections, contacts, and inclusions may reduce the visible complexity of a section. After Merge, the number of distinct intervals in I_n(ξ) is generally strictly less than 2^{n−2} and depends on ξ.

5.2. Why this is not a classical contractive IFS

The mappings F_k^± have coefficient of modulus 1. Therefore, for fixed non-zero offsets, this is an affine system of isometries, not a contractive IFS in the sense of Hutchinson theorem. Consequently, one cannot automatically speak of a fractal attractor or similarity dimension. The correct formulation is: finite order n is a finite orbit of the initial function d under a semigroup of affine isometries, followed by clipping and Merge.

5.3. Concrete paths to IFS generalization

A contractive version appears if normalized operators F_{k,λ}^±(r)=λ_k R_k±λ_k r with 0<λ_k<1 are introduced. Then each map has Lipschitz constant λ_k, and for sup λ_k<1 standard contractive IFS results apply. A second path is decreasing offsets R_k=R_0 λ^k: the sum of offsets is bounded by R_0/(1−λ), giving a natural estimate of the limiting radius. A third path is projection onto [0,M_max], which turns the dynamics into a bounded iteration on a compact set.

DOI: 10.5281/zenodo.20022183 Zenodo Publication
ORCID: 0009-0007-3657-2309
Date: 04.05.2026

$B_2=\{d\},\ B_{k+1}=\{R_k+r, R_k-r : r\in B_k\}$

$N_n=2^{n-2}$

$F_{k,\lambda}^{\pm}(r)=\lambda_k R_k \pm \lambda_k r,\ 0<\lambda_k<1$

$\Sigma_{k=0}^{\infty} R_0\lambda^k=R_0/(1-\lambda)$

Normalized IFS program

Introducing the normalization $F_{k,\lambda}^{\pm}(r)=\lambda_k R_k \pm \lambda_k r$ with $\lambda_k<1$ creates a contractive system to which classical theorems on an invariant compact set apply. This does not replace the finite-order construction but defines a separate limiting program.

For $R_k=R_0\lambda^k$ the sum of offsets is bounded, so the limiting radius can be estimated by a geometric series. For constant R_k such a compact limit usually does not exist without additional normalization.

DOI: 10.5281/zenodo.20022183 Zenodo Publication

ORCID: 0009-0007-3657-2309

Date: 04.05.2026

Chapter 6. Pseudoparaboloids of the 2nd, 3rd, and 4th orders

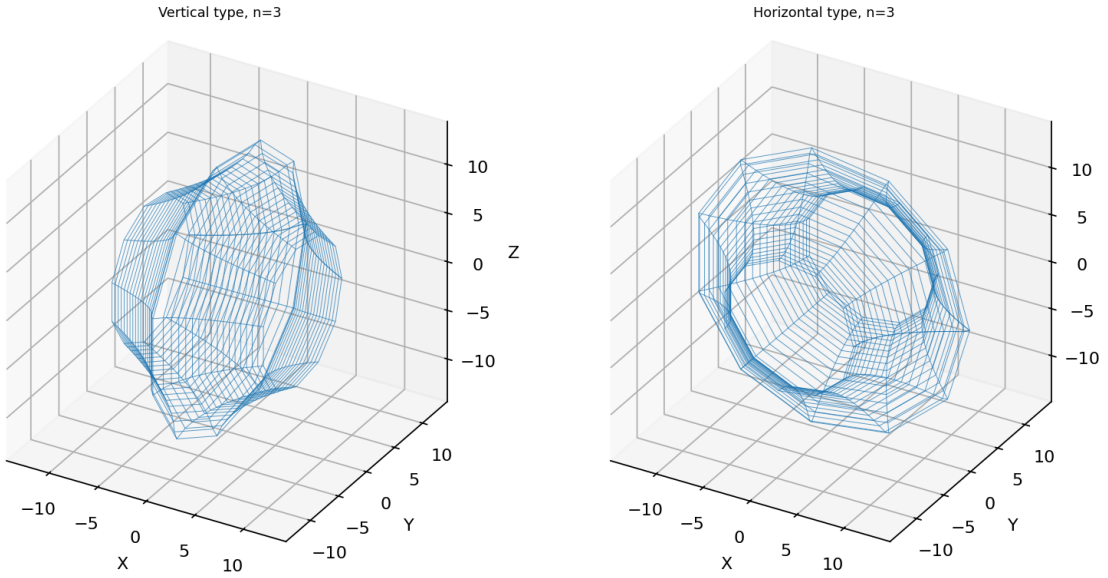

Fig. 7. 3D surfaces of the third order.

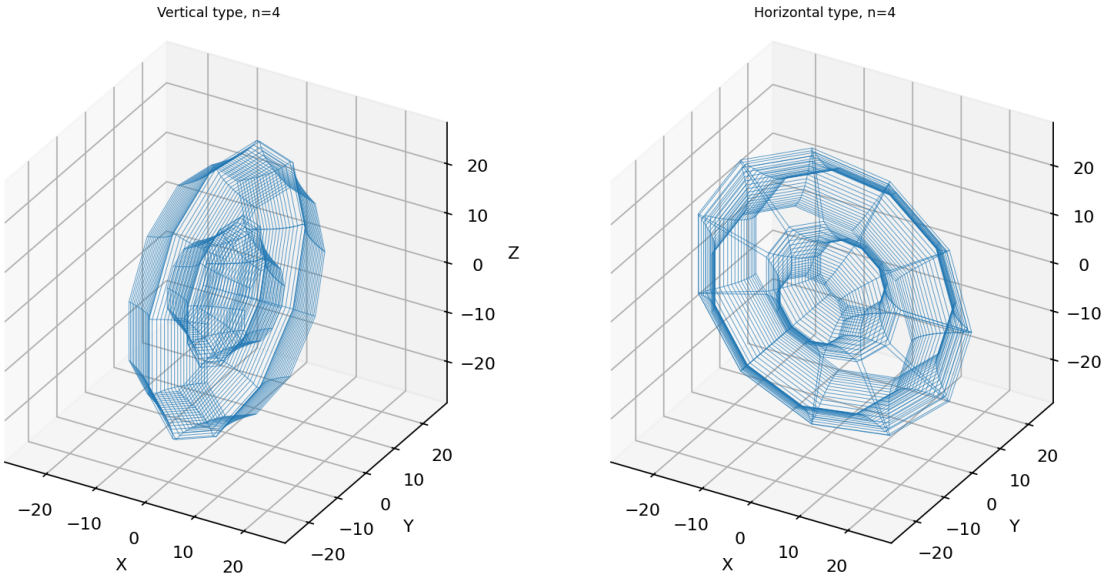

Fig. 8. 3D surfaces of the fourth order.

6.1. Second order

The second order is the base internal volume. It contains one radial interval [0,d(ξ)] and after rotation forms a domain reaching the axis of rotation. At this level there are no recursive offsets R_1,R_2,....

DOI: 10.5281/zenodo.20022183 Zenodo Publication

ORCID: 0009-0007-3657-2309 Date: 04.05.2026

6.2. Third order

The third order is generated by the first recursive offset R_1. For the base interval [0,d], before Merge the intervals [max(R_1−d,0),R_1] and [R_1,R_1+d] arise. They touch at R_1 and, for a single base interval, merge into one interval. At later levels, intervals with positive lower endpoints may create annular zones.

6.3. Fourth order and higher

The fourth order introduces the nested structure R_2±(R_1±d). Formally, four parabolic boundaries appear; after Merge the visible structure may be simpler. For n>4 the rule does not change: each new parameter acts on the entire result of the previous order, not again on the original generatrix.

$$I_3(\xi)=\mathrm{Merge}([\max(R_1-d,0),R_1]\cup[R_1,R_1+d])$$

$$B_4=\{R_2\pm(R_1\pm d)\}$$

Table 5. Orders and formal branches

Order	Offsets	Formal branches
2	none	1
3	R_1	2
4	R_1,R_2	4
n	R_1,…,R_{n−2}	2^{n−2}

Orders higher than the fourth

For n≥5 the rule does not change: each new recursive parameter acts on all intervals of the previous level. Therefore higher orders do not require new generatrix formulas, but require careful control of formal branches and Merge components.

DOI: 10.5281/zenodo.20022183 Zenodo Publication

ORCID: 0009-0007-3657-2309 Date: 04.05.2026

Chapter 7. Gaussian curvature of surfaces of revolution

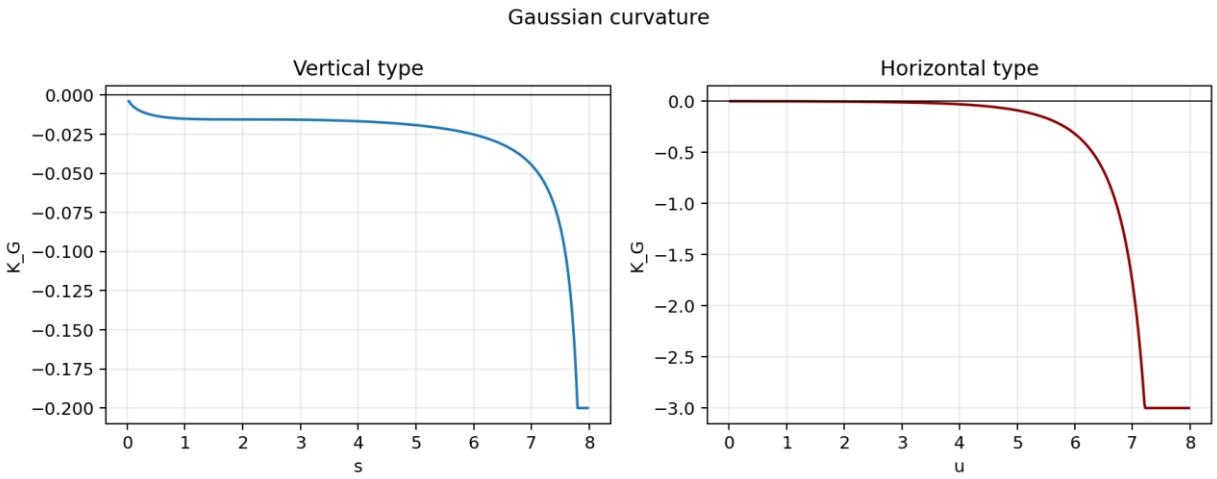

Fig. 9. Gaussian curvature of non-reflected base branches.

7.1. General formula

For a surface of revolution with radius ψ(ξ)>0, the Gaussian curvature of the lateral part is K_G=−ψ″/[ψ(1+ψ′²)^2]. The mean curvature is H=(1+ψ′²−ψψ″)/(2ψ(1+ψ′²)^{3/2}). These formulas apply only on smooth portions where ψ is twice differentiable and the radius is positive.

7.2. Vertical type

For s>0, ψ(s)=R−2√(fs), ψ′(s)=−√(f/s), and ψ″(s)=0.5√f/s^{3/2}. Therefore, on a non-reflected branch with ψ>0, K_G<0. As s→0+, ψ→R, ψ′²∼f/s, ψ″∼0.5√f/s^{3/2}; hence K_G∼−(0.5√f/s^{3/2})/[R(f/s)^2]=−(1/(2Rf^{3/2}))√s→0−. Thus the curvature tends to zero from the negative side, even though the derivative of the generatrix is unbounded.

7.3. Horizontal type

For u>0, ψ(u)=(R−u)^2/(4f), ψ′(u)=−(R−u)/(2f), and ψ″(u)=1/(2f)>0. Therefore, on a non-reflected branch, K_G<0 for 0<u<R. As u→R− the radius ψ→0 and K_G diverges to −∞, which is an axial singularity of the surface of revolution. At u=0, due to |u|, the derivative has a corner; analysis is performed piecewise from the left and the right.

7.4. Reflected branches

For arcs r=C−d, the sign of the second derivative changes, and the sign of K_G changes to the opposite. Therefore the full boundary of Ω_n is a piecewise composition of regions of negative and positive curvature. The correct statement is: the theory constructs pseudoparaboloid domains with controllable parabolic portions of variable curvature, among which non-reflected lateral branches have negative Gaussian curvature.

$$K_G = -\psi''/[\psi(1+\psi'^2)^2]$$

$$\psi_v'(s)=-\sqrt{(f/s)},\quad \psi_v''(s)=\sqrt{f}/(2s^{3/2})$$

$$\psi_h'(u)=-(R-u)/(2f),\quad \psi_h''(u)=1/(2f)$$

DOI: 10.5281/zenodo.20022183 Zenodo Publication

ORCID: 0009-0007-3657-2309 Date: 04.05.2026

Additional remarks

Curvature is not the only mechanism of a possible wave effect. In later modeling, boundary conditions, openness of the domain, material, scale relative to wavelength, and excitation method are simultaneously important. Therefore the sign of K_G is recorded as a geometric characteristic, not as sufficient physical proof of confinement.

When passing to higher orders, arcs of the form C+d and C−d must be analyzed separately. If the visible Merge boundary changes the active arc, curvature is a piecewise quantity and need not have a single sign over the whole object.

DOI: 10.5281/zenodo.20022183 Zenodo Publication

ORCID: 0009-0007-3657-2309 Date: 04.05.2026

Chapter 8. Singularities, smoothness, and surface area

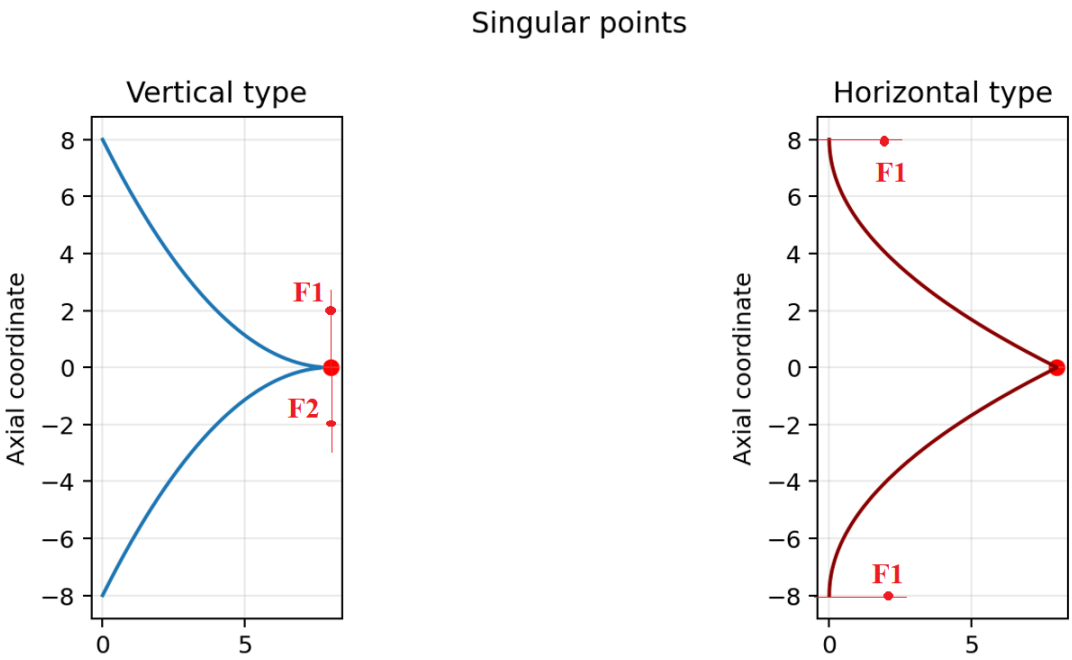

Fig. 10. Singular points of base generatrices.

8.1. Smoothness class

The boundary of Ω_n is piecewise smooth. On smooth parabolic arcs it is C^∞, but global C^1 smoothness may fail at vertices, contacts with the axis, and contact seams. Therefore Ω_n is correctly viewed as a compact domain with a piecewise smooth stratified boundary.

8.2. Surface area near a singularity

For a surface of revolution the lateral surface area is $S=\int 2\pi\psi\sqrt{(1+\psi'^2)}d\xi$. For the vertical branch as $s\to 0+$, $\psi\to R$ and $\sqrt{(1+\psi'^2)}\sim\sqrt{(f/s)}$. The integral $\int_0^\varepsilon 2\pi R\sqrt{(f/s)}ds$ is finite because $\int_0^\varepsilon s^{-1/2}ds=2\sqrt{\varepsilon}$. Thus the singularity at s=0 does not create infinite surface area.

In the horizontal type, as $u\to R-$ the radius ψ tends to zero and the derivative remains finite, so the area contribution is also finite. Mathematically, this allows such surfaces to be used as boundary domains after appropriate mesh treatment of singularities.

$$S=\int 2\pi\psi\sqrt{(1+\psi'^2)}d\xi$$

$$\int_0^\varepsilon s^{-1/2}ds=2\sqrt{\varepsilon}<\infty$$

Table 6. Singular points

Type	Point	Status
Vertical	s=0	unbounded derivative, finite area
Vertical	|s|=a	axis contact
Horizontal	u=0	corner due to |u|
Horizontal	|u|=R	axis contact, $K_G\to-\infty$ for C+d

DOI: 10.5281/zenodo.20022183 Zenodo Publication

ORCID: 0009-0007-3657-2309 Date: 04.05.2026

Chapter 9. Analytic foci of generating arcs

9.1. Derivation for the vertical type

Consider the right half-branch of the vertical type: $r=C+\varepsilon(R-2\sqrt{(fs)})$, $s\geq 0$. Shift the radial coordinate to the point $C+\varepsilon R$: $x_r=r-(C+\varepsilon R)=-2\varepsilon\sqrt{(fs)}$. Squaring gives $x_r^2=4fs$. This is the canonical parabola $x^2=4fs$ with axis along s and focus at distance f from the vertex. The two mirrored halves give $s=+f$ and $s=-f$. Transforming back gives $F_v(C,\varepsilon)=(C+\varepsilon R,\pm f)$.

9.2. Derivation for the horizontal type

For the horizontal type $r=C+\varepsilon(R-|u|)^2/(4f)$. On the half-axis $u\leq R$ set $y=R-u$. Then $r-C=\varepsilon y^2/(4f)$, or $y^2=4f\varepsilon(r-C)$. For $\varepsilon=+1$ the focus in local coordinates has radial coordinate $C+f$; for $\varepsilon=-1$ the opening direction is reversed and the coordinate becomes $C-f$. Since the vertices are at $u=\pm R$, the foci are $F_h(C,\varepsilon)=(C+\varepsilon f,\pm R)$.

$$r(\xi)=C_\sigma+\varepsilon_\sigma d(\xi)$$

$$F_v(C,\varepsilon)=\{(C+\varepsilon R,+f),(C+\varepsilon R,-f)\}$$

$$F_h(C,\varepsilon)=\{(C+\varepsilon f,+R),(C+\varepsilon f,-R)\}$$

Table 7. Foci of generating arcs

Type	Arc	Foci
Vertical	$C+\varepsilon d_v(s)$	$(C+\varepsilon R, \pm f)$
Horizontal	$C+\varepsilon d_h(u)$	$(C+\varepsilon f, \pm R)$

DOI: 10.5281/zenodo.20022183 Zenodo Publication

ORCID: 0009-0007-3657-2309 Date: 04.05.2026

Chapter 10. Area, volume, and quantitative functionals

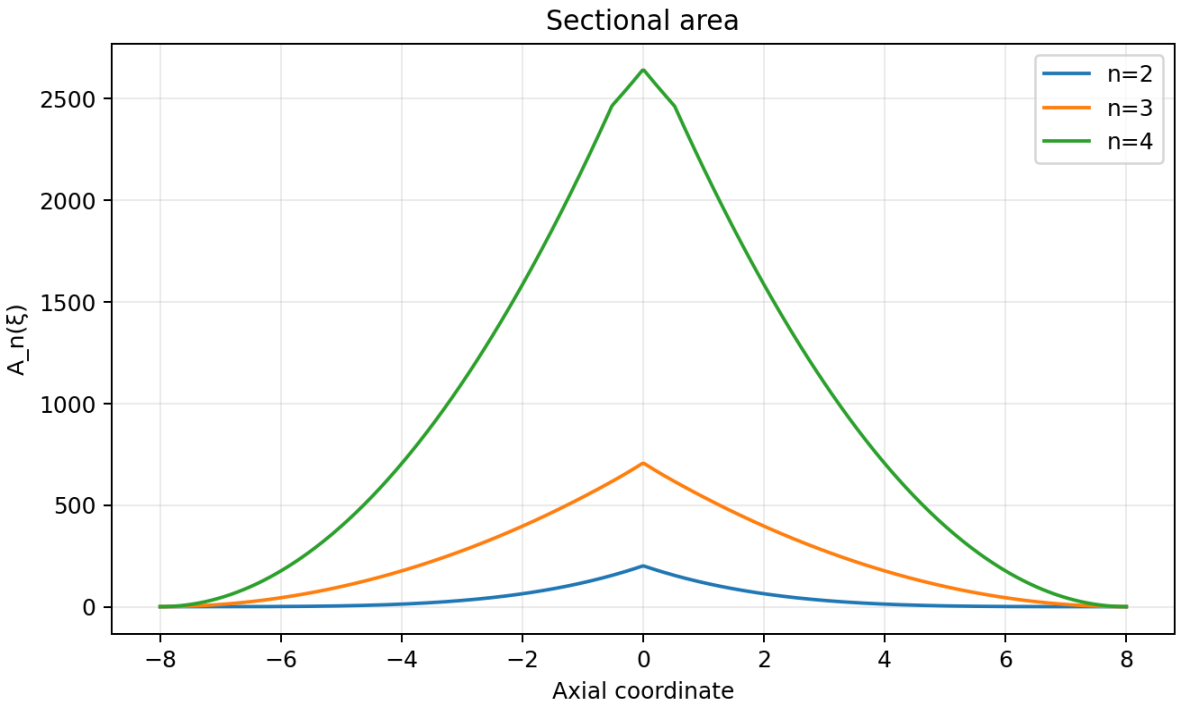

Fig. 11. Cross-sectional area as a function of axial coordinate.

10.1. Sectional area

At a fixed axial coordinate ξ, the canonical Merge set of intervals [α_j(ξ),β_j(ξ)] defines the cross-sectional area as a sum of disks or annuli. This quantity is important already in the geometric volume because it measures the distribution of internal volume along the axis.

10.2. Volume

The volume of a single object is V_n=∫A_n(ξ)dξ over the admissible axial domain. For a row system the volume does not exceed the sum of volumes of separate instances. For h<0 volumes overlap, and Merge removes only duplication of the common part, while preserving generating components as constructive elements.

$$A_n(\xi)=\pi\Sigma_j(\beta_j(\xi)^2-\alpha_j(\xi)^2)$$

$$V_n=\int_{D_n}A_n(\xi)d\xi$$

$$V_{n,m}\leq mV_n$$

DOI: 10.5281/zenodo.20022183 Zenodo Publication

ORCID: 0009-0007-3657-2309 Date: 04.05.2026

Chapter 11. Numerical reference example

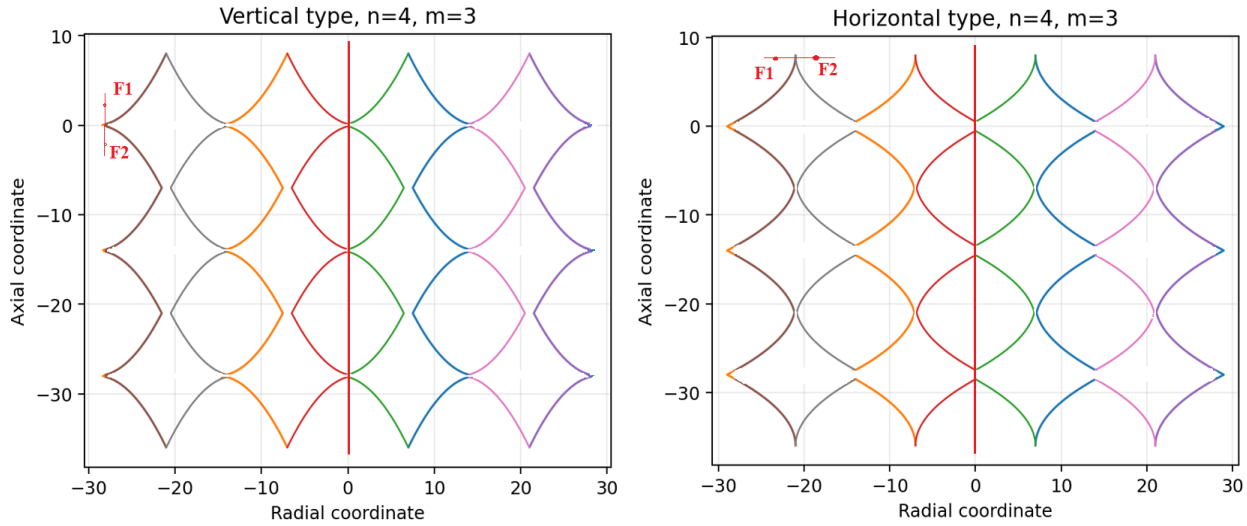

Fig. 12. Row system n=4, m=3, h=-2 in 2D.

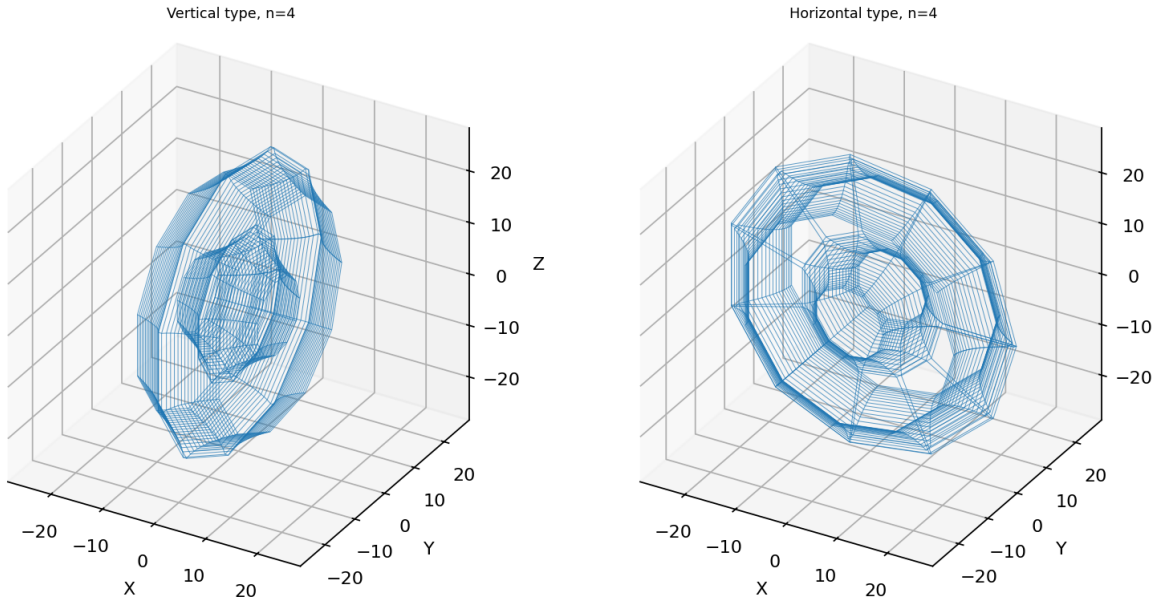

Fig. 13. Row system n=4, m=3, h=-2 in 3D.

11.1. Parameters of the example

As a reproducible reference, the parameter set f=2, R=8, a=R²/(4f)=8, R_1=7, R_2=14, n=4 is used. This example matches the parameters used in the final script as a base demonstration mode. It shows intersection/inclusion already at the first recursive step because R_1<M_0=8.

DOI: 10.5281/zenodo.20022183 Zenodo Publication

ORCID: 0009-0007-3657-2309 Date: 04.05.2026

11.2. Numerical values

The maximum radii by the estimate are M_0=8, M_1=R_1+M_0=15, and M_2=R_2+M_1=29. The formal number of fourth-order branches is N_4=2^(4−2)=4. At ξ=0 the interval after Merge is [0,29], and the sectional area is $\pi \cdot 29^2 \approx 2642.079$.

Step-by-step Merge verification at s=2.

For the vertical point s=2 one has d=R−2√(fs)=8−2√4=4, hence I_2(s=2)=[0,4].

Applying C_{R_1=7} gives [7−4,7]∪[7,7+4]=[3,7]∪[7,11], and because the intervals touch at 7, Merge gives I_3(s=2)=[3,11].

Applying C_{R_2=14} to [3,11] gives the difference interval [14−11,14−3]=[3,11] and the sum interval [14+3,14+11]=[17,25]. These intervals are separated, so I_4(s=2)=[3,11]∪[17,25], matching Table 8.

Table 8. Numerical example: intervals and areas

Point	d	Merge intervals n=4	A_n(ξ)
u=0 or s=0	8.000	[(0.0, 29.0)]	2642.079
u=4 (horizontal)	2.000	[(5.0, 9.0), (19.0, 23.0)]	703.717
s=2 (vertical)	4.000	[(3.0, 11.0), (17.0, 25.0)]	1407.434

Table 9. Foci of formal arcs n=4

Type	Focus coordinates
Vertical	[(-1.0, -2), (-1.0, 2), (13.0, -2), (13.0, 2), (15.0, -2), (15.0, 2), (29.0, -2), (29.0, 2)]
Horizontal	[(5.0, -8), (5.0, 8), (9.0, -8), (9.0, 8), (19.0, -8), (19.0, 8), (23.0, -8), (23.0, 8)]

Additional remarks

This example is a minimal check of all main formulas: base size a, formal branch number N_n, maximum radius M_n, intervals after Merge, sectional area, and analytic foci. It makes it possible to independently verify agreement between text, formulas, and script.

It is important that at ξ=0 Merge strongly simplifies the formal structure: four formal fourth-order branches yield one resulting interval [0,29]. At other ξ, separated annular zones appear, showing the difference between the formal branch tree and the actual radial domain.

Verification role of the example

The reference example shows that at ξ=0 the complexity of the formal tree may collapse into one interval, whereas at other ξ separated annular zones arise. This is a direct numerical confirmation of the need to distinguish B_n and I_n.

DOI: 10.5281/zenodo.20022183 Zenodo Publication

ORCID: 0009-0007-3657-2309 Date: 04.05.2026

Chapter 12. Row systems and the h parameter

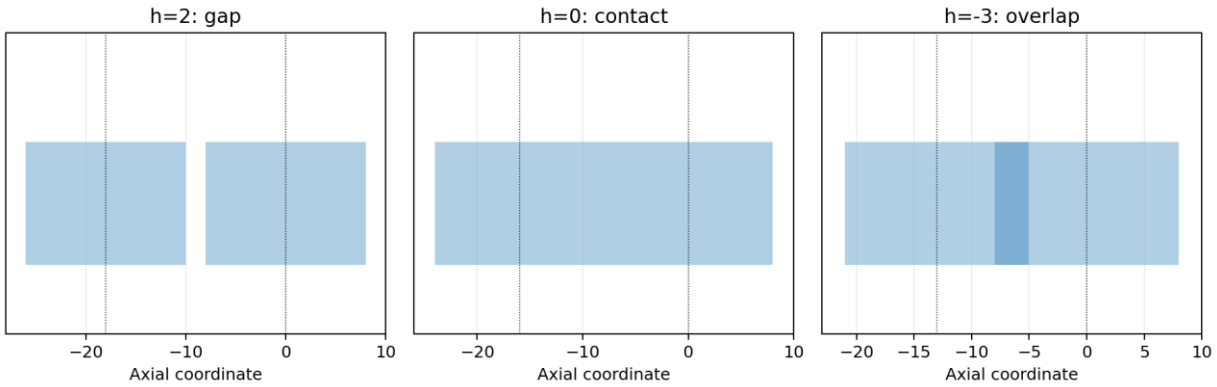

Fig. 14. Row assembly regimes by parameter h.

12.1. Step between rows

Row assembly is applied after constructing one instance Ω_n. If L is the half axial length of the selected type, the step between centers of neighboring instances is step=2L+h, and the shifts are Δ_j=−j(2L+h), j=0,…,m−1. In the present notation L=a for the vertical type, where $a=R^2/(4f)$, and L=R for the horizontal type, whose axial domain is $|u|\le R$. The parameter h does not change the internal order n; it controls the external axial assembly.

12.2. h>0, h=0, h<0

For h>0 there is a real gap between rows. For h=0 they touch at limiting points of the axial domain. For h<0 the axial supports overlap, and Merge constructs the unified volume without artificial connecting lines. This transition is geometric and must be validated separately in wave problems.

step=2L+h

Δ_j=−j(2L+h), j=0,…,m−1

Table 10. Row regimes

h	**Geometric meaning**
h>0	separate instances
h=0	contact
h<0	overlap and Merge

DOI: 10.5281/zenodo.20022183 Zenodo Publication

ORCID: 0009-0007-3657-2309 Date: 04.05.2026

Chapter 13. Program of further wave validation

14.1. Minimal set of physical tests

The transition from geometry to physics must be performed step by step. First, control geometries are compared: a cylinder, an ordinary paraboloid, a second-order pseudoparaboloid, then n=3, n=4, and row systems for h>0, h=0, h<0. For each domain, eigenfrequencies, modal volumes, Q-factors, energy distributions, confinement times, and fluxes through specified apertures must be computed.

14.2. Scientific position

Volume 1 establishes the constructive geometry and computational apparatus. The wave-level behaviour of waves of various physical nature in the domains Ω_{n,m} is a subject of the research programme to be addressed in subsequent volumes. The strength of the theory is that it defines a new parametric domain Ω_{n,m} on which these hypotheses can be tested reproducibly.

The title of reference [1] reflects the hypothesis of the broader research programme, not a wave-control result established in the present volume. The wave-validation programme will compare confinement and spectral behaviour in Ω_n and Ω_{n,m} with conventional photonic-crystal resonators [13], bound states in the continuum [14], whispering-gallery-mode microcavities [15], and coupled-resonator optical waveguides [16].

For electromagnetic validation, finite-element and finite-difference formulations should be benchmarked against standard references on Maxwell solvers [17] and FDTD methods [11]. For geometric limiting questions, the recursive construction may also be compared with standard references on measure, topology, and fractal geometry [18].

Table 11. Criteria for future validation

Criterion	Meaning
τ	energy confinement time
Q	quality factor
Spectrum	frequency shifts and splittings
Flux	directed output
V_mode	modal volume

DOI: 10.5281/zenodo.20022183 Zenodo Publication
ORCID: 0009-0007-3657-2309
Date: 04.05.2026

Conclusion

Final formulation

The theory of higher-order pseudoparaboloids introduces a reproducible geometric apparatus: base parabolic generatrices, interval recursion, Merge, row assembly, and the parameters f, R, R_k, n, m, h. In this apparatus the unified internal volume Ω_{n,m} becomes an independent object of design.

The geometric part is ready for further validation: properties of the domain, applicability limits, curvature, singularities, analytic foci, and quantitative functionals are defined. The next stage is not a new geometric declaration but physical modeling on the constructed domains.

DOI: 10.5281/zenodo.20022183 Zenodo Publication

ORCID: 0009-0007-3657-2309 Date: 04.05.2026

Appendix A. Notation and parameters

Table 12. Summary table of parameters

Symbol	Definition	Purpose
f	f>0	focal parameter
R	R>0	scale and focal-line distance
a	$R^2/(4f)$	base size
R_k	offsets	recursive levels
n	len(offsets)+2	order
m	integer ≥1	number of rows
h	real	axial gap/overlap
Ω_{n,m}	unified volume	computational domain

DOI: 10.5281/zenodo.20022183 Zenodo Publication

ORCID: 0009-0007-3657-2309

Date: 04.05.2026

Appendix B. References

[1] V. Khaustov. Geometric Wave Engineering: Pseudo-Surfaces of Variable Negative Gaussian Curvature as a Geometric Basis for Programmable Wave Control. (2026). DOI: 10.5281/ZENODO.19983291.

[2] V. Khaustov. Geometric wave engineering of ring-localized states in open pseudo-hyperbolic cavities. (2026). DOI: 10.5281/ZENODO.19944381.

[3] V. Khaustov. Higher-Order Pseudohyperboloids with the Merge Operation: A Geometric Foundation for Programmable Wave Confinement. (2026). DOI: 10.5281/ZENODO.19926174.

[4] Hutchinson J. E. Fractals and self-similarity. Indiana University Mathematics Journal. 1981;30(5):713-747.

[5] Falconer K. Fractal Geometry: Mathematical Foundations and Applications. Wiley, 2003.

[6] Barnsley M. F. Fractals Everywhere. Academic Press, 1988.

[7] do Carmo M. P. Differential Geometry of Curves and Surfaces. Prentice-Hall, 1976.

[8] Kreyszig E. Differential Geometry. Dover Publications, 1991.

[9] Morse P. M., Ingard K. U. Theoretical Acoustics. Princeton University Press, 1968.

[10] Jackson J. D. Classical Electrodynamics. Wiley, 1999.

[11] Taflove A., Hagness S. C. Computational Electrodynamics: The Finite-Difference Time-Domain Method. Artech House, 2005.

[12] Jin J. The Finite Element Method in Electromagnetics. Wiley, 2014.

[13] Joannopoulos J. D., Johnson S. G., Winn J. N., Meade R. D. Photonic Crystals: Molding the Flow of Light. Princeton University Press, 2008.

[14] Hsu C. W., Zhen B., Stone A. D., Joannopoulos J. D., Soljačić M. Bound states in the continuum. Nature Reviews Materials. 2016;1:16048.

[15] Vahala K. J. Optical microcavities. Nature. 2003;424:839-846. DOI: 10.1038/nature01939.

[16] Yariv A., Xu Y., Lee R. K., Scherer A. Coupled-resonator optical waveguide: a proposal and analysis. Optics Letters. 1999;24(11):711-713. DOI: 10.1364/OL.24.000711.

[17] Monk P. Finite Element Methods for Maxwell's Equations. Oxford University Press, 2003.

[18] Edgar G. A. Measure, Topology, and Fractal Geometry. 2nd ed. Springer, 2008.

[19] Marcuse D. Light Transmission Optics. Van Nostrand Reinhold, 1972.